Original Article

pISSN 2234-7518 • eISSN 2005-372X
http://dx.doi.org/10.4041/kjod.2012.42.4.169

THE KOREAN JOURNAL of ORTHODONTICS
KJO

A method for mandibular dental arch superimposition using 3D cone beam CT and orthodontic 3D digital model

Tae-Joon Park
Sang-Hyun Lee
Ki-Soo Lee

Department of Orthodontics, Graduate School, Kyung Hee University School of Dentistry, Seoul, Korea

Objective: The purpose of this study was to develop superimposition method on the lower arch using 3-dimensional (3D) cone beam computed tomography (CBCT) images and orthodontic 3D digital modeling. **Methods:** Integrated 3D CBCT images were acquired by substituting the dental portion of 3D CBCT images with precise dental images of an orthodontic 3D digital model. Images were acquired before and after treatment. For the superimposition, 2 superimposition methods were designed. Surface superimposition was based on the basal bone structure of the mandible by surface-to-surface matching (best-fit method). Plane superimposition was based on anatomical structures (mental and lingual foramen). For the evaluation, 10 landmarks including teeth and anatomic structures were assigned, and 30 times of superimpositions and measurements were performed to determine the more reproducible and reliable method. **Results:** All landmarks demonstrated that the surface superimposition method produced relatively more consistent coordinate values. The mean distances of measured landmarks values from the means were statistically significantly lower with the surface superimpositions method. **Conclusions:** Between the 2 superimposition methods designed for the evaluation of 3D changes in the lower arch, surface superimposition was the simpler, more reproducible, reliable method.
[Korean J Orthod 2012;42(4):169-181]

Key words: 3D cone beam CT image, Digital model, Superimposition, Mandibular arch

Received March 26, 2012; Revised June 5, 2012; Accepted June 7, 2012.

Corresponding author: Ki-Soo Lee.
Professor, Department of Orthodontics, Kyung Hee University School of Dentistry, 1 Hoegi-dong, Dongdaemoon-gu, Seoul 130-701, Korea.
Tel +82-2-958-9393 **e-mail** kislee@khu.ac.kr

The authors report no commercial, proprietary, or financial interest in the products or companies described in this article.

INTRODUCTION

It is important to estimate the changes in tooth position before and after orthodontic treatment to determine whether the teeth have been moved according to the anchorage requirements or to the planned tooth movement of the treatment objectives. Traditionally, the evaluation of tooth movement has been possible by superimposition of lateral cephalograms. However, cephalometric radiographs and superimpositions also present some disadvantages and limitations. The method can be technique sensitive and time-consuming while variable head positions in the cephalostat between serial radiographs may lead to errors in the comparison of treatment results. Most importantly, it is limited to 2-dimensional (2D) evaluation. Recent advances in computer technologies such as 3-dimensional (3D) computed tomography (CT), 3D surface scanning technology, computer-aided design, computer-aided manufacturing, and associated software have contributed not only to the precise diagnosis, treatment planning, and simulations, but also to the 3D evaluation of treatment results. Although these methods involve additional radiation exposure and time-consuming procedure, more accurate 3D data can be acquired.

On the maxillary dental arch, although little is known about the stability of identifiable landmarks on dental casts, palatal rugae has been suggested as relatively stable structures for registration of serial maxillary models.[1] The shape of the palatal vault and the medial portions of the palatal rugae are fairly stable throughout the development of the dentition.[2] The palatal rugae retain their shape and pattern throughout a person's lifetime.[3] Thus, they have been used for identification purposes in forensics.[4] Almeida et al.[5] and Bailey et al.[6] have studied the potential use of the palatal rugae for the superimposition of serial models and both studies concluded that specific parts of the palatal rugae (*e.g.*, medial) may be sufficiently stable to serve as anatomical references for superimposing serial maxillary models with headgear or premolar extraction treatment. Hoggan and Sadowsky[7] suggested that certain landmarks on the palatal rugae can be used as reliably as cephalometric superimpositions to assess anteroposterior molar movement.

Technical developments technology now permit the 3D superimposition of the maxillary dental arch using 3D model scanning technology. Ashmore et al.[8] reported that the method developed for the superimposition of digital configurations of serial dental models allowed accurate measurements of translational movement of the maxillary first-molar in 3 dimensions for both headgear and untreated groups. Miller et al.[9] reported that the digital superimposition of the maxillary arch was reproducible and that the error associated with using palatal rugae as reference landmarks may be similar to or less than that of current 2D cephalometric analyses.[10] Cha et al.[11] reported that use of a 3D digital orthodontic model superimposition technique on the maxillary dental arch

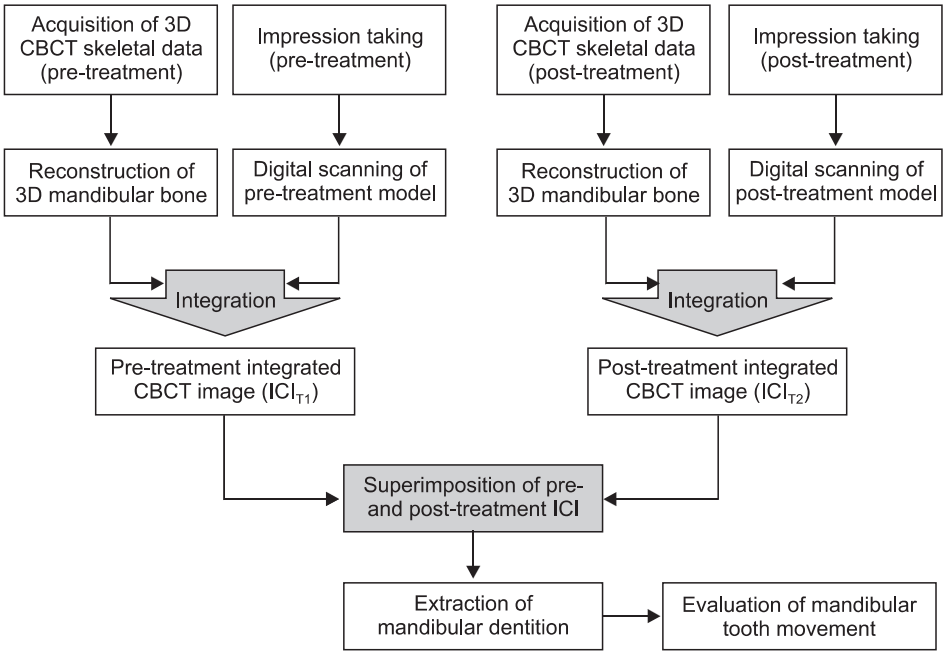

Figure 1. Overall procedure of the mandibular dental arch superimposition method. 3D, 3-dimensional; CBCT, cone beam computed tomography; ICI, integrated 3D CBCT image; T1, pre-treatment; T2, post-treatment.

http://dx.doi.org/10.4041/kjod.2012.42.4.169

was clinically as reliable as cephalometric superimposition for assessing orthodontic tooth movement.

However, none of these studies were performed on the mandibular dental arch since no well-known stable reference points or areas for superimposition have been established on the mandibular dental arch. No accurate and reproducible method has been introduced to date to evaluate the degree of 3D orthodontic tooth movement on the mandibular dental arch despite the available technology.

The purpose of this study was to introduce a method for mandibular dental arch superimposition in a non-gorwing patient by the combination of 3D cone beam CT data and 3D digital model data. The method was designed to use the basal bone area as the reference for superimposition while soft tissue or alveolar bone areas were avoided since they can be altered throughout orthodontic treatment. Two different registration methods for superimposing the mandible were designed to evaluate their reproducibility as well as practical applicability.

MATERIALS AND METHODS

One adult patient with no growth potency who had visited the Department of Orthodontics, Kyung Hee Dental Hospital and undergone orthodontic treatment, was examined. Cone beam computed tomography (CBCT) scan and alginate impression were taken on the same day prior to treatment, and in accordance with the patient's request, 1 day after debonding. Informed consent with the patient was received on the same day.

The superimposion system consisted of 6 main procedures: (1) acquisition of CBCT data, (2) acquisition of 3D digital model data, (3) integration of CBCT data and digital model data, (4) superimposition of pre-treatment and post-treatment integrated CBCT image, (5) extraction of the mandibular dentition portion, and (6) evaluation of tooth movement on the mandibular arch. The overall procedure for mandibular dental arch superimposition is shown in Figure 1.

Superimposition procedure

Step 1. Acquisition of 3D CBCT skeletal data and reconstruction of 3D mandibular bone images

Craniofacial skeleton 3D CBCT image data was acquired with an i-CAT imaging device (Imaging Sciences International, Hatfield, PA, USA). The patient underwent CBCT scanning in facial mode in 14-bit gray scale with 1.0 mm slice thickness, 1.0 mm voxel size, and image acquisition by single 360 degree rotation with a 40 s total scan time. The reconstructed digital data was directly transferred from the CBCT scanner to a personal computer and stored as digital imaging and communications in medicine (DICOM) files. Both pre-treatment and post-treatment DICOM data were transferred to Rapidform 2006 (INUS Technology Inc., Seoul, Korea), a 3D reverse-engineering software. The mandible was segmented by Rapidform 2006 from the craniofacial skeleton image (Figure 2).

Step 2. Acquisition of 3D digital model data by surface scanning

Orapix scanner; a 3D surface scanning system with a slit laser beam and non-contact measurement method (KOD-300, Orapix Co. Ltd., Seoul, Korea) was used to obtain 3D data from the dental cast model. The base of the digital model was fabricated similarly to the orthodontic diagnostic model. Both pre-treatment and post-treatment orthodontic 3D digital models are shown in Figure 3.

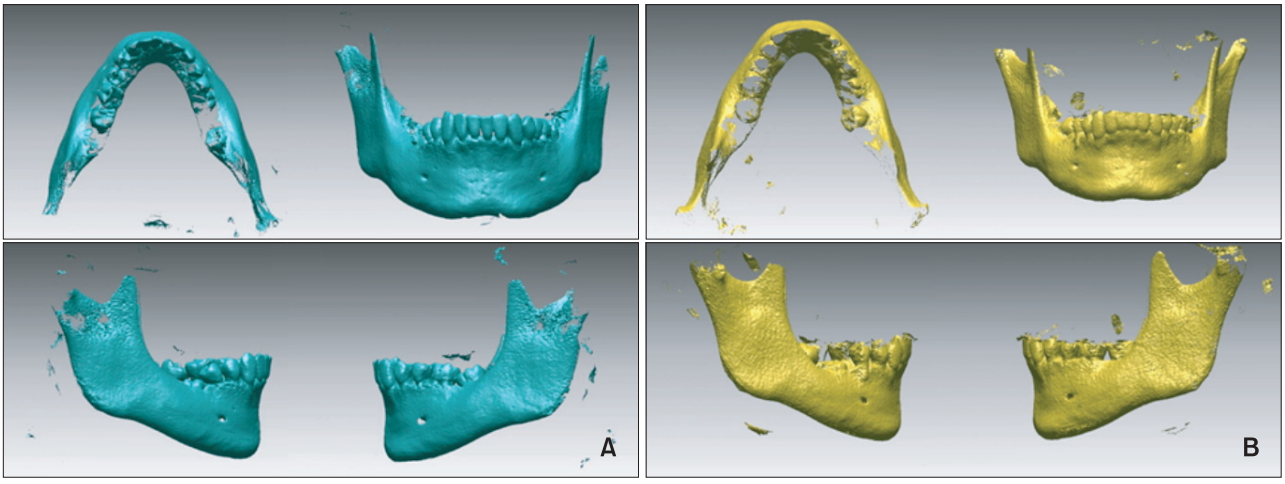

Figure 2. Reconstructed 3-dimensional image of the mandible. **A**, Pre-treatment; **B**, post-treatment.

 http://dx.doi.org/10.4041/kjod.2012.42.4.169

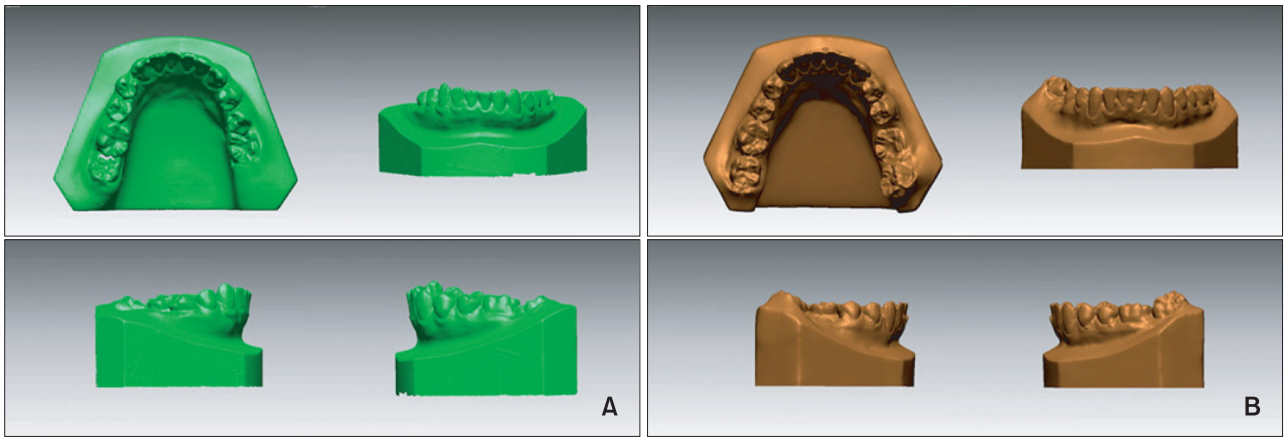

Figure 3. Orthodontic 3-dimensional digital model of mandibular dentition. A, Pre-treatment; B, post-treatment.

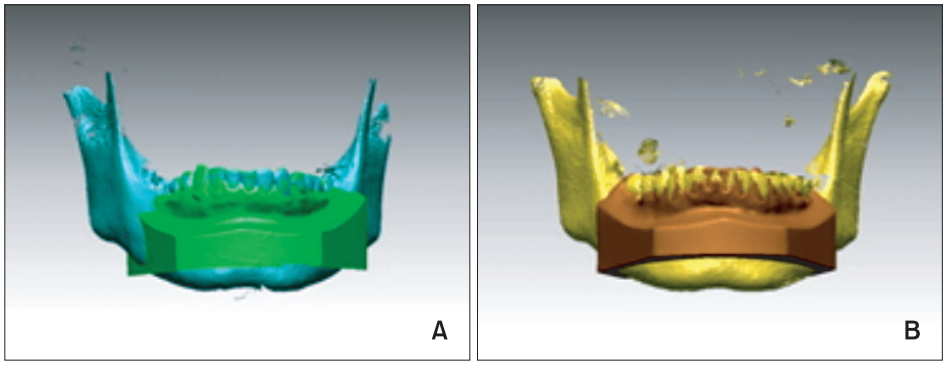

Figure 4. Preliminary fusion model by surface-to-surface matching (best-fit method). A, Pre-treatment; B, post-treatment.

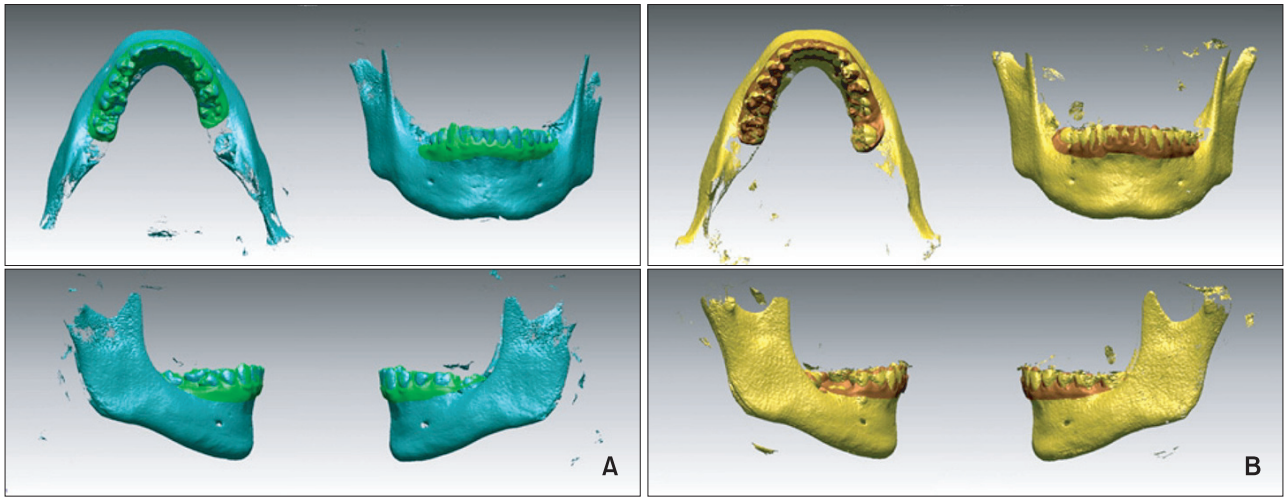

Figure 5. Final individual integrated 3D CBCT image of the mandible. A, Pre-treatment; B, post-treatment. 3D, 3-dimensional; CBCT, cone beam computed tomography.

http://dx.doi.org/10.4041/kjod.2012.42.4.169

Step 3. Initial integration of the mandible and mandibular dentition model

To create a preliminary fusion model, the dentition reconstructed by CBCT data was superimposed on the 3D digital model by a regional registration method.

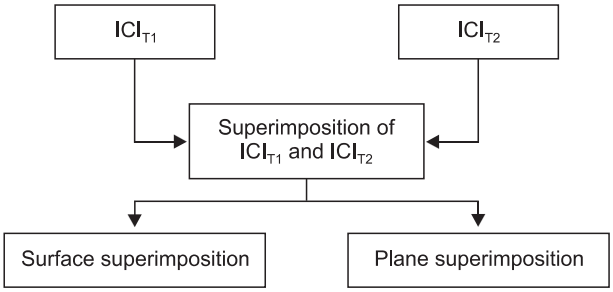

Figure 6. Two different registration methods designed for superimposing ICI$_{T1}$ and ICI$_{T2}$. ICI, Integrated 3D CBCT image; T1, pre-treatment; T2, post-treatment.

This function of Rapidform 2006, designated as 3D surface-to-surface matching (best-fit-method), employs a least-mean-squared algorithm.[12,13] According to the coordination between the tooth image from CBCT and the digitally scanned dental cast, the position, size, and posture of each tooth on the 3D digital model was automatically fitted to one of the subject's images of dentition in the CBCT data (Figure 4).

Finally, both pre- and post-treatment digital models were integrated into each mandible model, and the bases of the digital model superimposed on each image were removed. Thus, we produced individual integrated 3D CBCT images (integrated 3D CBCT image [ICI]$_{T1}$, ICI$_{T2}$) of the mandible, before and after the treatment, respectively, with an anatomical structure that included a digital model of higher resolution than the 3D CBCT image (Figure 5).

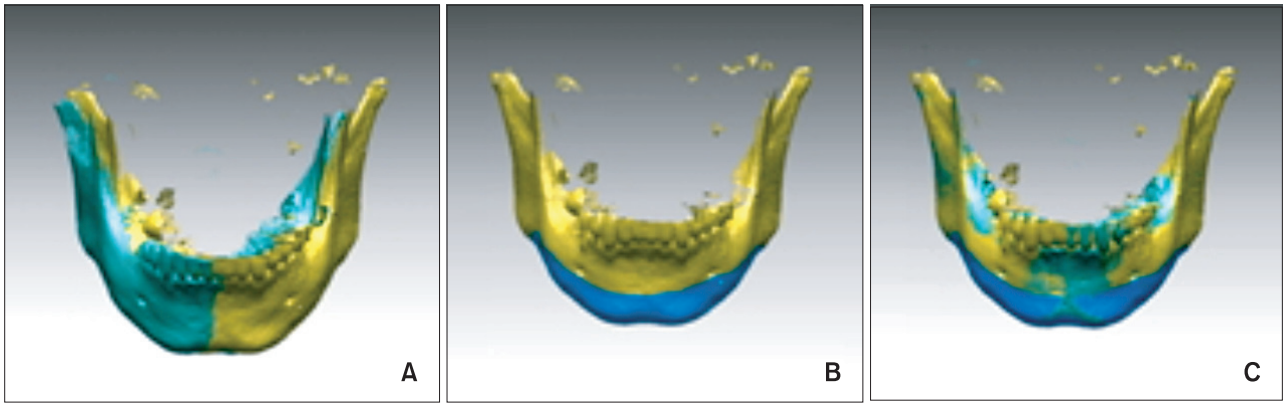

Figure 7. The procedure for surface superimposition. **A**, Selecting 2 ICI. **B**, Selecting the registration area (the inferior portion of mandible body and posterior portion of mandible ramus were selected). **C**, Superimposed ICI$_{T1}$ and ICI$_{T2}$ by surface-to-surface matching (best-fit method). ICI, Integrated 3D CBCT image.

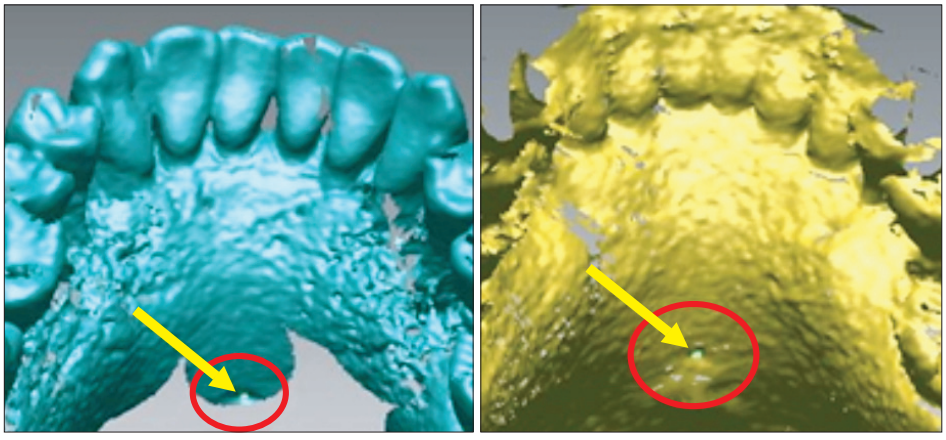

Figure 8. Aspect for the examination of lingual foramen. Arrows indicate the orifice of the lingual foramen.

http://dx.doi.org/10.4041/kjod.2012.42.4.169

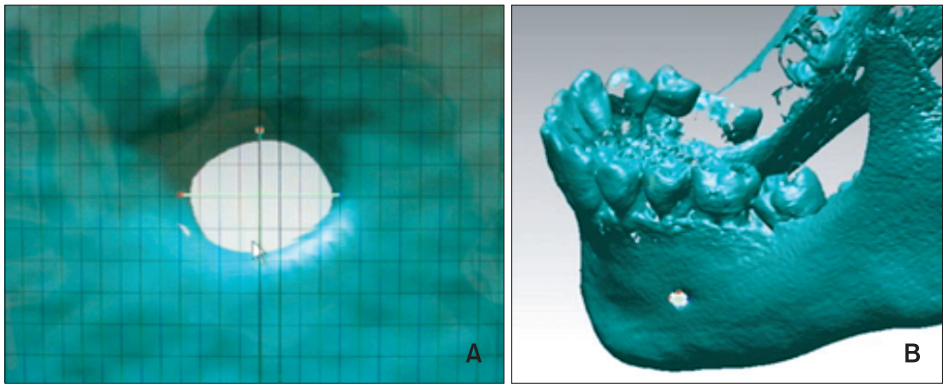

Figure 9. The center of the foramen was selected with a grid on the monitor by selecting 4 points of the foramen, the most superior, inferior and both lateral points, with the mandible rotated to give a perpendicular view to the foramen. Each procedure was performed on each mental foramen and lingual foramen on both ICI_{T1} and ICI_{T2}. ICI, Integrated 3D CBCT image; T1, pre-treatment; T2, post-treatment.

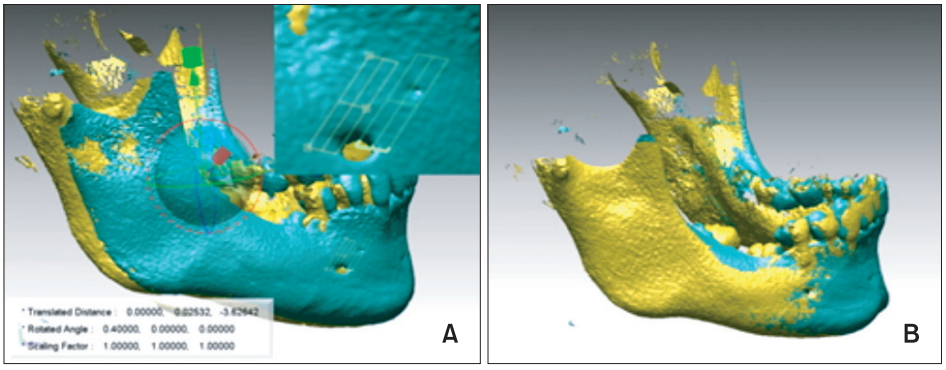

Figure 10. The procedure for plane superimposition. **A**, Selecting 2 ICI with the constituted plane. **B**, Superimposed ICI_{T1} and ICI_{T2} with the registration of 2 anatomical structure oriented planes. ICI, Integrated 3D CBCT image; T1, pre-treatment; T2, post-treatment.

Step 4. Superimposition of pre- and post-treatment ICI

Two different registration methods of superimposing ICI_{T1} and ICI_{T2} were used to evaluate their practical applicability and to estimate their reproducibility (Figure 6).

Surface superimposition

The first method designated as 'surface superimposition' was based on the surface of the basal bone structure of the mandible by surface-to-surface matching (best-fit method). The registration area was comprised of the basal bone structures of the mandible, which had not been altered by orthodontic treatment. The fully automated registration was computed by Rapidform 2006, with the limited manual process of selection and de-selection of the registration area. The inferior portion of mandibular body and the posterior portion of ramus were selected as the registration area. The procedure for surface superimposition is shown in Figure 7.

Plane superimposition

The second method, designated as plane superimposition was based on anatomical structure. The centers of both sides of mental foramen and the center of mandibular lingual foramen (a consistent arterial foramen in the middle of the mandible)[14,15] were selected as the landmarks. The center of each foramen was selected with a grid on the monitor by picking 4 points of the foramen - the most superior, inferior and both lateral points - with the mandible rotated to give a perpendicular view to the foramen (Figures 8 and 9). An anatomical structure-oriented plane was constituted with the selected 3 points. Subsequently, 2 planes constituted from ICI_{T1} and ICI_{T2} were superimposed by Rapidform 2006. The procedure for plane superimposition was shown in Figure 10.

Establishment of landmarks on dentition

Before the 2 superimposition procedures, reference points were established on the 3D image. The reference

http://dx.doi.org/10.4041/kjod.2012.42.4.169

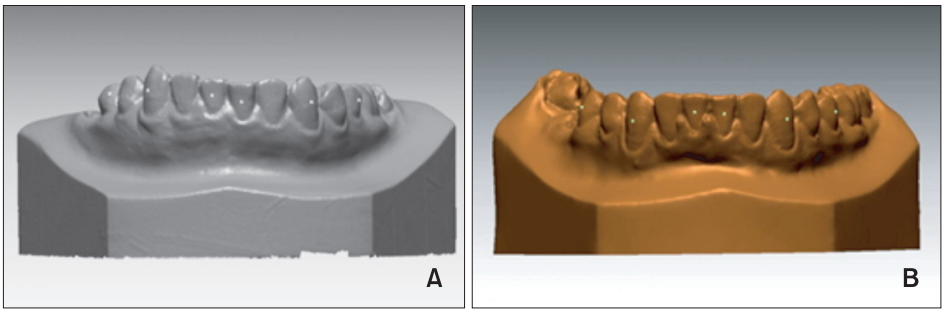

Figure 11. Facial axis points are marked on the lower central incisor, canine, and 2nd premolar on both left and right sides. White-spots indicate the marked points. **A**, Pre-treatment model; **B**, post-treatment model.

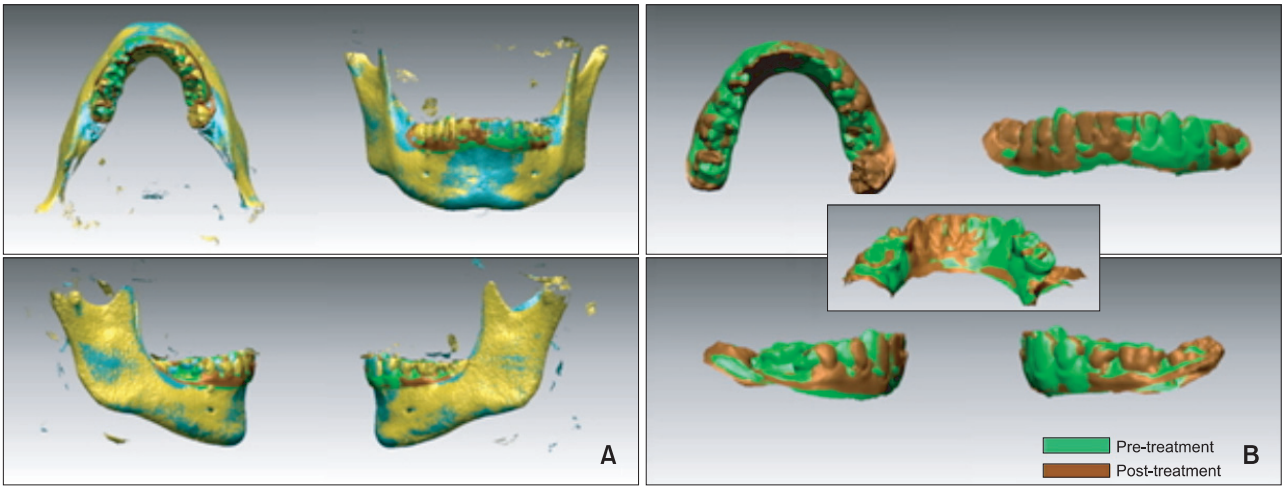

Figure 12. The dentition extracted from the superimposed image. **A**, Combined image, **B**, dentition was extracted.

points were the center of right and left mental foramen, the center of lingual foramen, the facial axis points[16] of right and left lower central incisors, canines, and 2nd premolars (Figure 11). Specially in this patient the mesiobuccal tip of the lower right 1st molar was also marked since it was found to be an ankylosed tooth.

Rapidform 2006 has a coordinate system, of which its origin is defined with the 0-point value by the software itself. The landmarks were established and selected on the 3D digital model image by 2 investigators using the Rapidform program. The points assignment was repeated 5 times each by each investigator, and the mean coordinate values of each landmark were used to define the final coordinate values. The final coordinate values (x, y, and z) of each landmark were transferred to Microsoft Office Excel 2007 (Microsoft, Redmond, WA, USA).

Step 5 and 6. Extraction of mandibular dentition

The dentition was extracted from the superimposed image (Figure 12), and the base of the model previously removed was added again on the dentition. The software easily performed the re-addition procedure at the same position since the bases were previously constructed on the digital model. Finally, the superimposed 3D mandibular dental arch was ready to be used for evaluation of the orthodontic tooth movement that occurred throughout treatment.

Statistical analysis

The initially established landmarks consisted of 10 points on both pre- and post-treatment images. After applying the 2 methods of superimposition, the coordinate values (x, y, z) of the same landmarks were transferred to Microsoft Office Excel 2007. Each method of superimposition was performed 30 times to estimate reproducibility (steps 4 to 6) and all the coordinate values of post-treatment landmarks after each superimposition were transferred to Microsoft Office Excel 2007.

First, the mean values and variances of each x-, y-, and z-coordinate values of the post-treatment landmarks were calculated with both the surface superimposition and plane superimposition methods. The equality of variance

 http://dx.doi.org/10.4041/kjod.2012.42.4.169

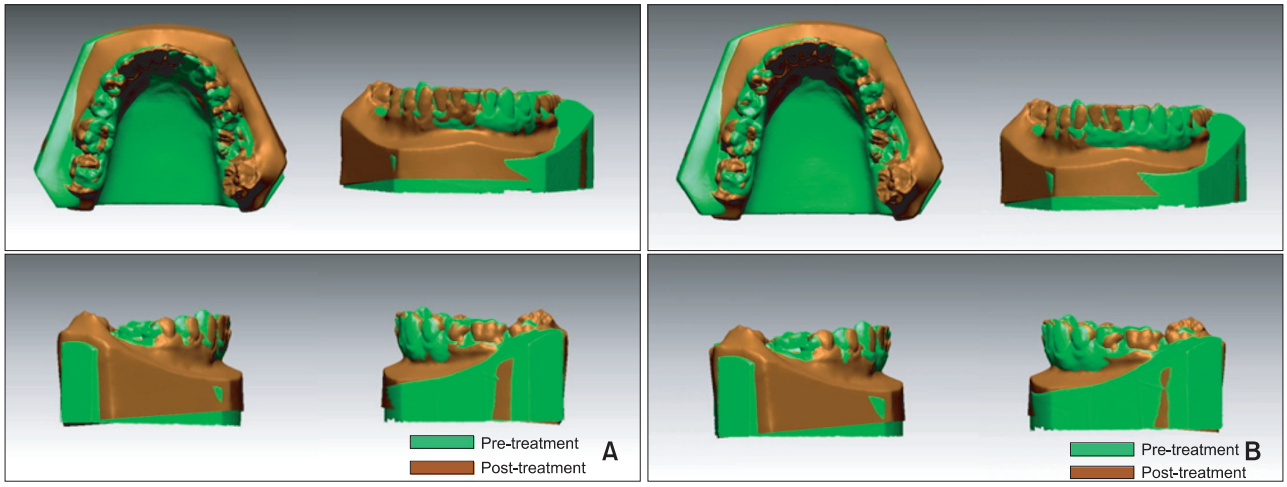

Figure 13. Final image of superimposed mandibular dental arch. **A**, By surface superimposition; **B**, by plane superimposition.

test was carried out for each x-, y-, and z-coordinate values as a scalar with Matlab 7.5 (Minitab Inc., State College, PA, USA). The null hypothesis and alternative hypothesis were expressed as H0: $\delta_p^2 < \delta_s^2$ and Ha: $\delta_p^2 > \delta_s^2$ (H0: null hypothesis, Ha: alternative hypothesis, δ_p^2: variance of plane superimposition, δ_s^2: variance of surface superimposition). The difference in variance between the 2 superimposition methods was 0 at a significance level of 0.05.

Then the mean distance (mean value of the distance from the mean coordinate value of the 30 trials to the coordinate values of each trial) was calculated for both methods with Matlab. Student's t-test was performed to determine whether a significant difference existed between the mean distances of the 2 superimposition methods for each landmark using SAS 9.1 (SAS Institute Inc., Cary, NC, USA). The null hypothesis was rejected at a significant level of 0.05.

To compare the stability of the reproduced results from both surface and plane superimposition, the following 2 methods were used, since the data used for the analysis involved 3D coordinates, and no appropriate method for the precise comparison of 2 different superimposition methods has been established.

At first, 3D coordinates were divided into x, y, z axes and the variance for results from each superimposition method was calculated in each axis. Subsequently, *F*-test for equal variances was used to compare variance values, and the difference in distance between values from each trial and the mean values of the 2 superimposition methods were compared.

RESULTS

Superimposition of the mandibular dental arch was achieved with 2 designated methods. Final superimposed 3D digital models were produced (Figure 13) to permit the evaluation of tooth movement visually as well as numerically.

The reproducibility of the methods was first compared with the equality of variance test. The results are shown in Table 1. Twenty-eight coordinate values demonstrated statistically significant differences ($p < 0.05$) between the variance of each method, indicating that the plane superimposition method generated more variability in coordinate values after each trial. The values of each trial were marked 3-dimensionally using the Matlab program. Figure 14 shows a scatter plot of coordinate values on the x - y, y - z, and z - x axis of the lower left incisor, which demonstrated a large variation in the coordinate values (x: $F = 59.3$, $p < 0.001$, y: $F = 11.61$, $p < 0.001$, z: $F = 491.16$, $p < 0.001$) after each trial between the 2 methods.

Student's t-test revealed a statistically significant difference ($p < 0.001$) in the mean distance from the mean coordinate value of each landmark to the corresponding coordinate value of each trial, indicating that the surface superimposition method had relatively more consistent coordinate values closer to the mean on all landmarks (Table 2).

DISCUSSION

Many 3D instruments enable orthodontists to acquire 3D images of the facial structures, including both hard and soft tissues. Not only the 3D visualization of the structures but also the measurements and comparison of different evaluation times have been made possible. With advances in technology, 3D superimposition with 3D digital models on the maxillary arch has been developed with reliable reference areas for superimposition. In

http://dx.doi.org/10.4041/kjod.2012.42.4.169

Table 1. Equality of variance test between the two methods

Lanmark	Coordinate value	*F*-ratio	*p*-value
Right mental foramen (RMF)	x	2.07	0.028*
	y	7.10	0.000‡
	z	5.07	0.000‡
Left mental foramen (LMF)	x	2.09	0.026*
	y	2.45	0.009†
	z	2.88	0.003†
Lingual foramen (LF)	x	3.23	0.001†
	y	1.64	0.095
	z	19.35	0.000‡
Lower left incisor (LL1)	x	59.31	0.000‡
	y	11.61	0.000‡
	z	491.16	0.000‡
Lower left canine (LL3)	x	10.75	0.000‡
	y	11.89	0.000‡
	z	12.85	0.000‡
Lower left 2nd premplar (LL5)	x	3.58	0.000‡
	y	15.24	0.000‡
	z	1.97	0.037*
Lower right incisor (LR1)	x	13.44	0.000‡
	y	12.71	0.000‡
	z	502.17	0.000‡
Lower right canine (LR3)	x	5.80	0.000‡
	y	27.15	0.000‡
	z	7.90	0.000‡
Lower right 2nd premolar (LR5)	x	7.59	0.000‡
	y	6.10	0.000‡
	z	1.24	0.287
Lower right 1st molar (LR6)	x	8.08	0.000‡
	y	16.91	0.000‡
	z	11.65	0.000‡

*$p < 0.05$; †$p < 0.01$; ‡$p < 0.001$.

recent years CT has been adopted for 3D virtual surgical planning and simulation of post-operative outcomes in orthognathic surgery with various registration methods for superimposition.[17-20] This study aimed to introduce a reproducible superimposition technique for the mandibular dental arch by the generating integrated 3D CBCT images based on CBCT scans and 3D surface scanning data with improved imaging quality of the dentition. This study was limited to a non-growing patient who did not undergo an orthognathic surgical procedure to exclude the effects of mandibular growth or surgical change from the evaluation and comparison of the reproducibility of the 2 designed methods.

CBCT was selected as the device for CT scanning for several reasons; it provides orthodontists with a new modality for research and permits vertical scanning of patients in a normal seated position. Ferrario et al.[21] reported that 3D measurement values were not sensitive to head posture. In this study, the patient underwent CBCT scanning with a slice thickness of 1.0 mm, which improved the visual quality of 3D reconstruction. Further improvement is possible with a smaller slice thickness, but this change would also result in increased image size, requiring greater computational power and longer user interaction time.

Recently, a computerized composite skull model was introduced to orthognathic surgery,[22] which eliminated the need for plaster casts to create digital models since a laser surface scanner subsequently scans the impressions of the dentition. Thus, one potential source of errors that reduces the accuracy of the complete system appears to have been removed. However, specialized radiolucent dental impressions trays with fiducial markers are needed to allow for the registration of the dental arches assessed by CT and laser scans. This technique introduces new sources of error, because several additional steps accompanying the data acquisition and registration procedures are required. Therefore, in this study we chose a simpler approach using a plaster cast scanned with an Orapix scanner for the registration of the CBCT scans and the 3D dental surface images.

Extremely accurate modeling of the facial structures can be achieved with 3D reconstruction of CT-derived images. However, it is not possible to ascertain whether dental morphology can be acquired as accurately with this technique due to artifacts from metallic restorations. Moreover, intercuspation during occlusion leads to overlapping images, resulting in inaccurate morphology of the individual tooth. The resultant effect on the CT images appears as pronounced dark and bright streaks, non-linear edge gradients, and sampling errors arising from the surface restoration.[23] Swennen et al.[24] discussed the drawbacks of CT imaging; it does not provide detailed surface dental morphology or precise intercuspation data due to its limited resolution, and the interocclusal relationship is often obscured by radio-opaque dental restorations or orthodontic brackets.

Combining 3D CBCT images and the 3D virtual model data can compensate for these issues. Gateno et al.[22] introduced a technique to integrate digital models into a virtual 3D CT bone model of the skull. Measurements acquired from using 3 mm titanium spheres as markers demonstrated high accuracy (0.1 - 0.5 mm) in the study of

 http://dx.doi.org/10.4041/kjod.2012.42.4.169

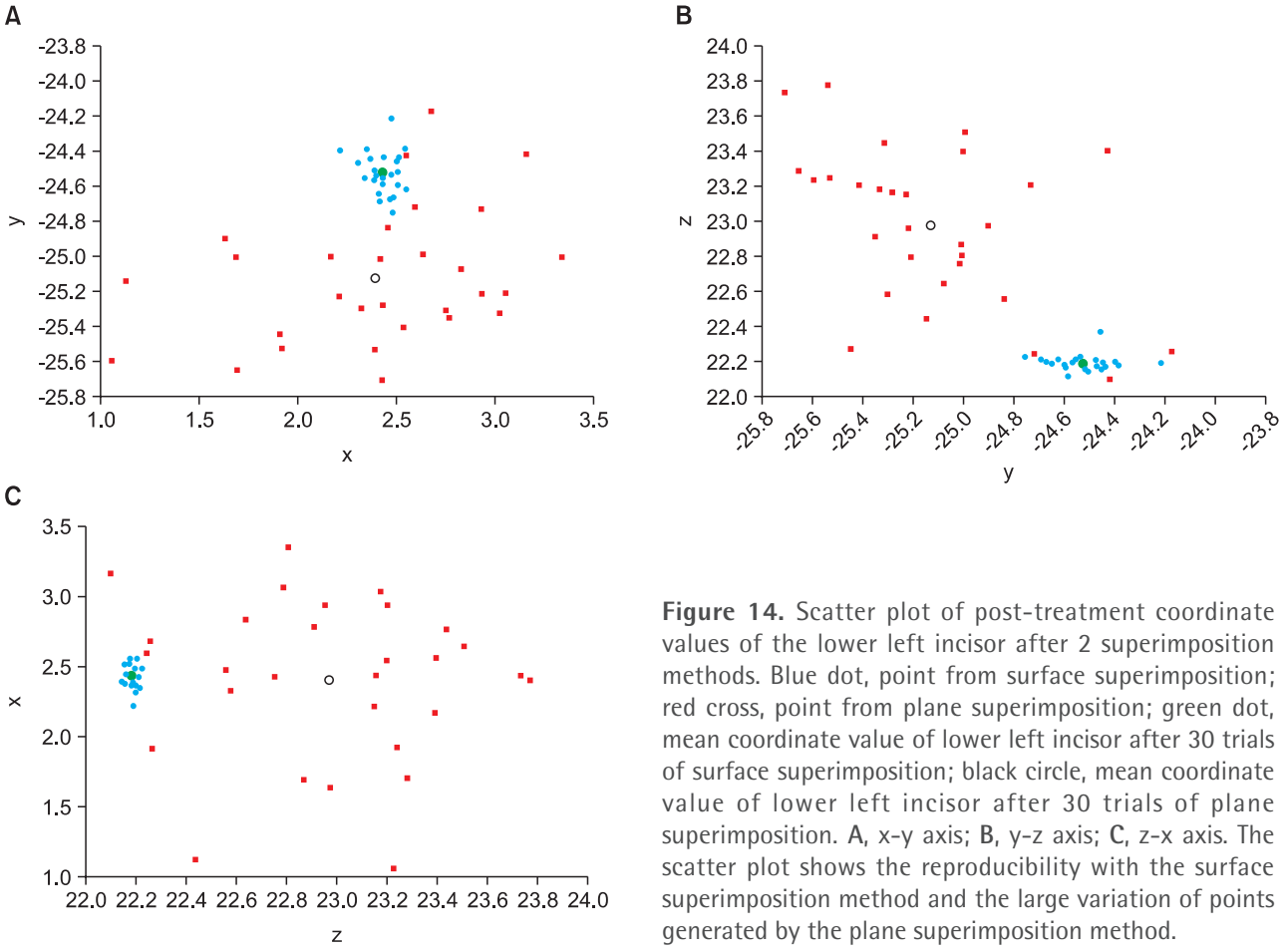

Figure 14. Scatter plot of post-treatment coordinate values of the lower left incisor after 2 superimposition methods. Blue dot, point from surface superimposition; red cross, point from plane superimposition; green dot, mean coordinate value of lower left incisor after 30 trials of surface superimposition; black circle, mean coordinate value of lower left incisor after 30 trials of plane superimposition. A, x-y axis; B, y-z axis; C, z-x axis. The scatter plot shows the reproducibility with the surface superimposition method and the large variation of points generated by the plane superimposition method.

Table 2. Three-dimensional mean distance

Landmark	Distance (mm)								t-value	*p*-value
	Surface superimposition				Plane superimposition					
	Mean	SD	Min	Max	Mean	SD	Min	Max		
Right mental foramen (RMF)	0.508	0.221	0.247	1.262	0.952	0.392	0.378	1.975	5.40	0.0000†
Left mental foramen (LMF)	0.577	0.336	0.075	1.596	0.890	0.456	0.113	1.986	3.02	0.0037*
Lingual foramen (LF)	0.361	0.191	0.078	0.835	0.653	0.337	0.108	1.358	4.13	0.0001†
Lower left incisor (LL1)	0.109	0.072	0.014	0.313	0.724	0.332	0.240	1.445	9.90	0.0000†
Lower left canine (LL3)	0.270	0.111	0.038	0.535	0.873	0.489	0.272	2.370	6.59	0.0000†
Lower left 2nd premplar (LL5)	0.506	0.247	0.096	1.205	0.973	0.417	0.254	1.728	5.27	0.0000†
Lower right incisor (LR1)	0.222	0.141	0.018	0.566	0.979	0.365	0.457	2.185	10.59	0.0000†
Lower right canine (LR3)	2.265	0.129	0.179	0.562	0.852	0.361	0.182	1.767	8.40	0.0000†
Lower right 2nd premolar (LR5)	0.386	0.196	0.064	0.889	0.786	0.329	0.298	1.498	5.72	0.0000†
Lower right 1st molar (LR6)	0.249	0.135	0.022	0.576	0.934	0.360	0.377	1.658	9.76	0.0000†

SD, Standaed deviation; Min, minimum; Max, maximum.
*$p < 0.01$; †$p < 0.001$.

a single dry skull. Nkenke et al.[25] suggested a considerable progress in the fusion of images from different imaging modalities using software-based approaches in which 2 modalities are combined and mounted in a single

http://dx.doi.org/10.4041/kjod.2012.42.4.169

coordinate system. Combining CT with optical 3D imaging seems to be a reasonable approach to correct metallic artifacts, allowing precise assessment of the tooth surface and accurate simulation of the post-operative dental occlusion. In a single patient, accuracy levels of 0.66 and 0.56 mm for the mandible and maxilla, respectively, with a modified double CT scan procedure resulted in accurate registration, with registration error of 0.1355 ± 0.0323 mm, and analysis of variance of 0.0564 mm.[24]

Two known methods for the registration of CT data and scanned optical dental images have been setablished: point-based registration of external fiducial markers[22,26] and surface-based registration of anatomical structures.[25] We used surface-based registration referred to as regional registration with surface-to-surface matching (best-fit method), which included a least square technique. This approach is advantageous in that it can be applied with no additional fiducial markers, which in turn require more additional time-consuming procedures that may also introduce new sources of error. Although their study did not assess a combination technique for CT and dental images, Cha et al.[11] evaluated the accuracy of measurements by calculating the superimposition discrepancies between pre- and post-treatment 3D models in the maxillary arch. Surface-to-surface matching (best-fit method) resulted in a mean error of 0.0399 mm, standard error of 0.0289 mm, and standard deviation of 0.1583 mm, which the authors concluded as a satisfactory accuracy level.

Subsol et al.[27] proposed methods that have guided the progress of our study, in which semi-landmarks on the surface were used to incorporate information about vectors in the vicinity of the landmark. The landmarks were established and selected on the 3D digital model images 5 times each by 2 investigators. The mean coordinate values of each landmark were used to define the final coordinate values. The determined landmarks were then fixed to the image so as not to be changed during the superimposition procedure, and the coordinate values were then determined after every superimposition procedure for a total of 30 repetitions with each method.

In this study, we introduced 2 methods for superimposing ICI, designated as surface superimposition and plane superimposition. The surface superimposition method was designed for automation by applying in-house computer tools. Plane superimposition was designed to include more information concerning anatomical structures in the superimposition procedure. The landmarks used - mental foramen and lingual foramen - are known as relatively stable structures on the mandible. In a study of 314 dried mandibles, McDonnell et al.[28] reported that the lingual foramen present in 311 specimens (99.04%), and that the wall of the canal, not the genial tubercles, produced the radio-opacity peripheral to the foramen seen on radiographs. Although the authors remarked that the foramen was not seen on many radiographs of the lower incisor region, a change in orientation of the x-ray beam could account for this discrepancy. In this study, the registration plane was oriented to the 3 points of these structures that were considered stable.

The superimposition procedure itself was performed 30 times with each method. Reproducibility was evaluated based on the dispersion of samples represented by sample variance. A lower variance of samples from one method compared to the other, indicates that the method is relatively more efficient in terms of reproducibility. However, in the present study each sample was a series of 3D-vectors, resulting in a covariance matrix for each method instead of a scaler variance. Therefore, we decomposed these series of vectors into 3 series of scalars using x, y, and z coordinates and then used the *F*-test to determine whether 2 samples from these 2 methods had the same variance. The Surface method demonstrated a lower sample variance than the plane method within a 5% significance level at 28 coordinates. We attempted to express the magnitude of the 3D vector while excluding the directional component. The mean distance from the mean coordinate value of each landmark was measured for both methods. Student's t-test revealed a statistically significant difference in the mean distance between the 2 methods and also indicated that the surface superimposition method had a relatively more consistent distribution closer to the mean coordinate values over 30 trials. Therefore, the surface method was considered to provide more reproducible results after repeated trials. This reproducibility of the surface superimposition method was helped by our negligible observer variability, which allowed image analysis procedures largely independent of observer errors. By contrast, the relative inconsistency of plane superimposition is thought to result from the procedure, which requires manual selection of the anatomical structures that could generate inter- or intra-observer variability. Cevidanes et al.[29] introduced a fully automated superimposition method using voxel-wise rigid registration of the cranial base, as the cranial base structures are not altered by surgery. This technique represents an advance from the processe described by Kawamata et al.,[30] who used an observer-dependent method to superimpose and rotate the post-surgery CT until anatomical landmarks overlapped these same structures in the pre-surgery semi-transparent model. Our results also show improved reproducibility with the automated superimposition technique (surface superimposition), which minimizing the possibility of observer errors. Because it is almost fully computerized except for the selection process of the registration area, it avoids human error, thereby simplifying the process and producing

 http://dx.doi.org/10.4041/kjod.2012.42.4.169

integrated images with a high degree of reproducibility in positioning. Therefore, surface superimposition method may be more precise and convenient method for mandibular surface model superimposition.

The stability of reproduced results from both surface and plane superimposition were compared statistically. The data used for the analysis involved 3D coordinates, and no appropriate method for the precise comparison has been established. As alternatives, the following 2 methods were used. First, 3D coordinates were divided into x, y, and z axes and the variances for each result from both superimposition methods was calculated on each axis. The *F*-test for equal variances was then used to compare the values of variance, and a conclusion was drawn by comparing this calculated *F* value to the critical value of *F* distribution (alpha = 0.05) since the *F* value is known to demonstrate *F* distribution under conditions of the null hypothesis. Second, the difference in distance between the results and mean points that were generated by the 2 superimposition methods were compared. For this aim, mean x, y, and z values were deduced from 3D coordinates, and the distances of each result from the corresponding mean values were calculated. Then the mean distance distribution and mean values that were generated from the 2 superimposition methods were analyzed. The null hypothesis was that the mean distance calculated by plane superimposition was less than or equal to that calculated by surface superimposition. The alternative hypothesis was that the mean distance calculated by plane superimposition was greater than that calculated by surface superimposition. Standard deviation of the test statistic t is known to demonstrate t-distribution under the conditions of the null hypothesis. Therefore, a conclusion was drawn by comparing the t value calculated as described above and the ctitical value of t-distribution (alpha = 0.05).

Future studies should include more patient samples for the superimposition procedures for reproducibility and also a comparison with the measurement of tooth movement detected on the conventional cephalographs. This study was limited to a non-growing patient, and more studies may be needed to reflect the growth changes of the mandible during superimposition. The true methodological error of the superimposition system was not estimated in this study, and such an estimation would be challenging because the mandible is an independent structure with a joint on the craniofacial skeleton. However, the error of registration and the reproducibility of the 2 methods were determined. Because significant changes in mandibular position can occur during orthodontic treatment, such as autorotation of the mandible, condylar displacement, and centric occluson/centric relation discrepancy, the registration reference in this study was designed within the mandible itself, not on craniofacial structures. Additionally, the registration reference was based on the basal bone of the mandible, which, in contrast to soft tissues or alveolar bone, had not been altered by orthodontic tooth movement. Therefore, this method is assumed to meet the submillimetric accuracy requirements of orthodontic tooth movement in non-growing patients. It is expected to gain acceptance as the new method helps patients to better understand the 3D changes in the mandibular dental arch throughout the treatment process.

CONCLUSION

The visualization of 3D superimposition and measurements can help orthodontists to better evaluate treatment outcomes. Here, we introduced 2 methods for 3D mandibular dental arch superimposition; surface superimposition and plane superimposition. The surface superimposition method demonstrated more reliable and reproducible results based on its minimization of the possibility of observer errors. These findings suggest that 3D mandibular dental arch superimposition can be achieved using the surface superimposition method.

REFERENCES

1. van der Linden FP. Changes in the position of posterior teeth in relation to ruga points. Am J Orthod 1978;74:142-61.
2. Lebret L. Growth changes of the palate. J Dent Res 1962;41:1391-404.
3. Peavy DC Jr, Kendrick GS. The effects of tooth movement on the palatine rugae. J Prosthet Dent 1967;18:536-42.
4. English WR, Robison SF, Summitt JB, Oesterle LJ, Brannon RB, Morlang WM. Individuality of human palatal rugae. J Forensic Sci 1988;33:718-26.
5. Almeida MA, Phillips C, Kula K, Tulloch C. Stability of the palatal rugae as landmarks for analysis of dental casts. Angle Orthod 1995;65:43-8.
6. Bailey LT, Esmailnejad A, Almeida MA. Stability of the palatal rugae as landmarks for analysis of dental casts in extraction and nonextraction cases. Angle Orthod 1996;66:73-8.
7. Hoggan BR, Sadowsky C. The use of palatal rugae for the assessment of anteroposterior tooth movements. Am J Orthod Dentofacial Orthop 2001;119:482-8.
8. Ashmore JL, Kurland BF, King GJ, Wheeler TT, Ghafari J, Ramsay DS. A 3-dimensional analysis of molar movement during headgear treatment. Am J Orthod Dentofacial Orthop 2002;121:18-29.
9. Miller RJ, Kuo E, Choi W. Validation of Align Technology's Treat III digital model superimposition tool and its case application. Orthod Craniofac Res

http://dx.doi.org/10.4041/kjod.2012.42.4.169

2003;6(Suppl 1):143-9.
10. Ghafari J, Baumrind S, Efstratiadis SS. Misinterpreting growth and treatment outcome from serial cephalographs. Clin Orthod Res 1998;1:102-6.
11. Cha BK, Lee JY, Jost-Brinkmann PG, Yoshida N. Analysis of tooth movement in extraction cases using three-dimensional reverse engineering technology. Eur J Orthod 2007;29:325-31.
12. Commer P, Bourauel C, Maier K, Jäger A. Construction and testing of a computer-based intraoral laser scanner for determining tooth positions. Med Eng Phys 2000;22:625-35.
13. McDonagh S, Moss JP, Goodwin P, Lee RT. A prospective optical surface scanning and cephalometric assessment of the effect of functional appliances on the soft tissues. Eur J Orthod 2001;23:115-26.
14. Goaz PW, White SC. Oral radiology; Principles and interpretation. 2nd ed. Toronto: Mosby; 1987. p. 189-90.
15. Kasle MJ. An atlas of dental radiographic anatomy. 3rd ed. Toronto: Saunders; 1989.
16. Andrews LF. Straight wire: The concept and appliance. San Diego: L.A. Wells; 1989 .
17. Girod S, Keeve E, Girod B. Advances in interactive craniofacial surgery planning by 3D simulation and visualization. Int J Oral Maxillofac Surg 1995;24:120-5.
18. Chen LH, Chen WH. Three-dimensional computer-assisted simulation combining facial skeleton with facial morphology for orthognathic surgery. Int J Adult Orthodon Orthognath Surg 1999;14:140-5.
19. Motohashi N, Kuroda T. A 3D computer-aided design system applied to diagnosis and treatment planning in orthodontics and orthognathic surgery. Eur J Orthod 1999;21:263-74.
20. Xia J, Samman N, Yeung RW, Shen SG, Wang D, Ip HH, et al. Three-dimensional virtual reality surgical planning and simulation workbench for orthognathic surgery. Int J Adult Orthodon Orthognath Surg 2000;15:265-82.
21. Ferrario VF, Sforza C, Poggio CE, Serrao G. Facial three-dimensional morphometry. Am J Orthod Dentofacial Orthop 1996;109:86-93.
22. Gateno J, Xia J, Teichgraeber JF, Rosen A. A new technique for the creation of a computerized composite skull model. J Oral Maxillofac Surg 2003;61:222-7.
23. Svendsen P, Quiding L, Landahl I. Blackout and other artefacts in computed tomography caused by fillings in teeth. Neuroradiology 1980;19:229-34.
24. Swennen GR, Barth EL, Eulzer C, Schutyser F. The use of a new 3D splint and double CT scan procedure to obtain an accurate anatomic virtual augmented model of the skull. Int J Oral Maxillofac Surg 2007;36:146-52.
25. Nkenke E, Zachow S, Benz M, Maier T, Veit K, Kramer M, et al. Fusion of computed tomography data and optical 3D images of the dentition for streak artefact correction in the simulation of orthognathic surgery. Dentomaxillofac Radiol 2004;33:226-32.
26. Nishii Y, Nojima K, Takane Y, Isshiki Y. Integration of the maxillofacial three-dimensional CT image and the three-dimensional dental surface image. Orthod Waves 1998;57:189-94.
27. Subsol G, Thirion JP, Ayache N. A scheme for automatically building three-dimensional morphometric anatomical atlases: application to a skull atlas. Med Image Anal 1998;2:37-60.
28. McDonnell D, Reza Nouri M, Todd ME. The mandibular lingual foramen: a consistent arterial foramen in the middle of the mandible. J Anat 1994;184:363-9.
29. Cevidanes LH, Bailey LJ, Tucker GR Jr, Styner MA, Mol A, Phillips CL, et al. Superimposition of 3D cone-beam CT models of orthognathic surgery patients. Dentomaxillofac Radiol 2005;34:369-75.
30. Kawamata A, Fujishita M, Nagahara K, Kanematu N, Niwa K, Langlais RP. Three-dimensional computed tomography evaluation of postsurgical condylar displacement after mandibular osteotomy. Oral Surg Oral Med Oral Pathol Oral Radiol Endod 1998;85:371-6.

 http://dx.doi.org/10.4041/kjod.2012.42.4.169